

Au AND Cu NANOPARTICLES AND CLUSTERS SYNTHESIZED BY PULSED LASER ABLATION: EFFECTS OF POLYETHYLENIMINE (PEI) COATING

M. Á. GRACIA-PINILLA^{a,b*}, M. VILLANUEVA^c, N. A. RAMOS DELGADO^d,
M. F. MELÉNDREZ^f, J. MENCHACA-ARREDONDO^a.

^a*Facultad de Ciencias Físico Matemáticas, Universidad Autónoma de Nuevo León, Ciudad Universitaria, San Nicolás de los Garza, Nuevo León, 66450, México.*

^b*Centro de Investigación en Innovación y Desarrollo en Ingeniería y Tecnología, Universidad Autónoma de Nuevo León, PIIT, Apodaca, Nuevo León, 66600, México.*

^c*Facultad de Ciencias Químicas, Universidad Autónoma de Nuevo León, Ciudad Universitaria, San Nicolás de los Garza, Nuevo León, 66450, México.*

^d*Instituto Tecnológico de Nuevo León, Centro de Investigación e Innovación Tecnológica, Guadalupe, Nuevo León, 67170. México.*

^f*Hybrid Materials and Polymers Laboratory (HMPL), Department of Materials Engineering (DIMAT), Faculty of Engineering, University of Concepcion, 270 Edmundo Larenas, Casilla 160-C, 4070409 Concepcion, Chile.*

Au and Cu nanoparticles (NPs) and clusters were synthesized in aqueous media by nanosecond pulsed laser ablation (NPLA) through the irradiation of light of wavelength of 1064 nm produced by a Nd:YAG laser at a fluence of 20 mJ/cm² per pulse and of pulses of 5 ns. The study of the effects of the polyethyleneimine (PEI) on the Au and Cu-NPs and clusters was also performed. The capping process was performed during the irradiation of the Au or Cu targets using the laser. The procedure allows for a remarkably low range of particle sizes on the sample between 0.5 nm and 10 nm, with an average of 5 nm. The addition of the polymer (PEI) in the aqueous media inhibits the formation of aggregates or the coalescence process of the NPs, and it also produces Au-PEI and Cu-PEI clusters with sizes smaller than 2 nm; in both cases, narrow size distributions were validated by HRTEM and zeta potential (ZP) analysis. The high crystallinity (five-fold preferential orientation) of the Au-NPs-PEI(**capping**) compared with Au-NPs without PEI was also evidenced by microscopy analysis. Finally, a new route to produce Au-NPs, Cu-NPs and clusters functionalized with PEI was proposed.

(Received August 6, 2014; Accepted October 20, 2014)

Keywords: Nanoparticles, pulsed laser ablation, clusters, controlled growth.

1. Introduction

In recent years, nanoscience and nanotechnology have become major scientific fields; the importance of these research fields is based on the new properties of materials enabled by structures of size in the nanometric scale. Materials of this type can be useful in many applications, such as optical sensors, gas sensors, biomedical sensors, chemical catalysis, electronic devices and optoelectronic devices, among others [1 -5]. Size-controlled synthesis of nanoparticles is a significant step in the development of novel nanotechnology applications because the potential applications and their efficiency strongly depend on the following parameters: *i*) high size control, *ii*) compositional control, *iii*) geometry control and *iv*) the grade of the dispersion [6-11]. Today, it

*Corresponding author: miguel.graciapl@uanl.edu.mx

is conceivable to design nanomaterials with high performance through the optimal control of these parameters, which would enable the design of interesting new devices.

Several techniques has been used for the preparation of metallic nanoparticles (NPs), the most common of which is typically called wet chemistry, involving the reduction of metal ions to metal atoms in the presence of various complex or stabilizer agents (thiols, organic acids, amines and others) and subsequently obtaining a partial or total capping of metallic nanoparticles. Through this technique, it is possible to control the aggregation of metallic nanoparticles; examples of these techniques include Sol-Gel, impregnation, solvo-thermal, co-reduction and dendrimer-encapsulated, among others[12-15]. In contrast, physical methods are based in the atomization or vaporization of the metals, obtaining the purest materials. Metallic particles and complex oxides compounds can be synthesized by sputtering, physical vapor deposition (PDV), laser ablation and inert gas condensation (IGC), among other techniques [6, 11, 16-18]. The principal advantage of these techniques is the high reproducibility; however, new requirements on the characteristics of the nanoparticles are emerging, such as size selection, dispersion degree, surface functionalization, preferential geometry and, in the case of alloys, the degree of A-B segregation or mixing. These parameters are more relevant for metal nanoparticles due to the exceptional optical, electrical, catalytic, magnetic and antiviral properties of metal nanoparticles in the range on 1-20 nm. Moreover, particles with sizes of less than 2 nm (approximately 100 atoms) exhibit different behavior with respect to those of larger sizes because their diverse properties depend more on the number constituents atoms of the surface. In this case, these particles are commonly called clusters or atomic assemblies, and all of their properties can be changed by adding a single atom and also by changing its electrical charge (positive, negative or neutral), the principal property in these particles is the high surface/volume ratio of greater than 50% and hence, the high surface energy [19-23].

The major challenge in any of these synthesis methods is avoiding the coalescence process, which is required because the physical and chemical properties of metallic nanoparticles change due to agglomeration or flocculation. To address this issue of coalescence, many authors [24-26] proposed different synthesis paths, such as the use of organic and inorganic capping ligands and the control of the density, among others. The type of ligand that can bind to the nanostructures depends on the polarity media and the final application of the nanoparticles. Polymer capping ligand are also used because they have a non-toxic surface, in contrast with those organic capping ligands that have groups thiols in their structure [19], and because of the possibility of modification of the surface polarity layer by layer. Polyethyleneimine can be used as both a reductant and a stabilizer agent in the synthesis. PEI capping is the most common capping approach for biological and biomedical applications [27-31].

The use of pulsed laser ablation in water media is a new route for the synthesis of metallic nanoparticles; many research groups have reported the synthesis of a diverse array of metallic nanoparticles and obtained different results [32-36]. Our work is focused on the PEI *in situ* capping study of metallic nanoparticles during the time the laser irradiates the target. The capping effect stabilizes the atoms controlling the nucleation and growth process. In this work, the optimal size and the shape control of the synthesis of Au-NPs and Cu-NPs are determined. In addition, with good thermodynamic and chemical environment control, one can verify the nucleation and aggregation process (which are conducted mainly by reduction of Gibbs free energy) of the nanoparticles and clusters with PEI capping.

Au-NPs and Cu-NPs are useful materials for producing conductive patterns in the electronics industry (Kawasaki et al 2011), but their high stability is required; to address the aerobic oxidation and coalescence process, many authors suggest that it is difficult to control the stability, quality and shape control of these nanoparticles. In the present work, we describe a new route for the synthesis of Au-NPs and Cu-NPs and clusters of uniform size and shape, with and without PEI capping, using a nanosecond pulsed laser radiation in water media. This development opens a new path to designed metallic nanomaterials of ideal shape, size and modified surface to be used in optical, catalytic, biomedical applications or other applications where nano-properties are relevant. The study of the polymer effect on nanoparticles was performed in two sets: 1) Au-NPs and Cu-NPs synthesis without PEI capping and 2) Au-NPs and Cu-NPs synthesis with PEI

capping. Both experiments were performed under identical experimental conditions, as described below.

2. Experimental

2.1 Synthesis

In the synthesis process, the metallic nanoparticles were produced in deionized water (18.2 Mohm cm) media. The laser ablation was performed using a nanosecond (Nd:YAG) laser, which delivers 5 ns full-width half-maximum (fwhm) pulses (wavelength: 1064 nm and 532 nm; repetition rate: 10 Hz; beam diameter: 6 mm). The laser beam was focused by a convex lens with a focal length of 100 mm onto a sample (Au or Cu sputtering target in 50 mL of deionized water) [35] contained in a Pyrex glass container of 100 mL. The output energy of the laser was constant at 20 mJ/cm², and the ablation time was 15 min.

The effect of the polymer capping on nanoparticles was studied by two consecutive experiments, the first was the synthesis of Au-NPs without PEI capping and the second corresponded to the synthesis of Au nanoparticles with PEI capping [Au-NPs-PEI(capping)]. Both experiments were performed with the same parameters described previously.

2.2 Characterization

(i) Transmission electron microscope (TEM) imaging studies and selected area electron diffraction (SAED) were performed using a 2100F JEOL TEM operated at 200 kV (point resolution of 0.19 nm) to record HRTEM images, and a FEI TITAN G2 80-300 operated at 300 kV was used. Au- and Cu-NPs without capping and with capping were dropped (previously treated in an ultrasonic bath) onto a carbon-coated copper grid and dried at room temperature. (ii) UV-Vis spectroscopy was conducted using a Beckman DU 640 Spectrophotometer (Beckman Coulter) over the spectral range of 330-800 nm. Cells with a 1-cm path length of quartz were used in these analyses. The spectra were recorded at room temperature in deionized water. (iii) Dynamic light scattering (DLS) was performed in a Nanotracc Wave particle size analyzer (Microtrac) over a size range from 0.8 nm to 6.5 nm; the analyzer can also perform zeta potential measurements. All of the samples were analyzed at room temperature.

2.2.1 Structural Study

The Au-NPs and Cu-NPs dispersed in the aqueous solution were dropped onto TEM grids; the nanoparticles with capping were prepared in the same manner. Some TEM results are shown in Fig. 1; in these high-magnifications images, which are very clear, the surface interface region can be seen between the CuO and the Cu-NPs. In the upper right corner in Fig. 1a, there is a zone that corresponds to CuO (ICDD reference code 00-001-1117), which has a monoclinic structure with planes (111) of interplanar distance of 0.23 nm. The same figure also showed Cu-NPs with cubic structure (ICDD reference code 00-001-1242) and crystalline planes (200) of interplanar distance of 0.18 nm. The results indicated the low stability of Cu-NPs without PEI capping and the oxidation of these Cu-NPs to copper (II) oxide. This oxidation is due to the high reactivity of the Cu-NPs surface; a similar behavior was found for other metals (Ti to TiO₂) in environmental conditions [37]. The method used in the synthesis is very energetic; therefore, it is possible that the high energy of the laser promotes the reaction quickly to obtain nanoparticles. This method is easy, fast and can be extrapolated by changing the target. The disadvantages of this method are that some metallic nanoparticles can coalesce, aggregate and oxidize in an aqueous solution, when the reactions are conducted without any organic polymers as the capping agent. In summary, one can perform this reaction using other solvents and capping agents, such as ethylene glycol, PVP and CTAB. All of this effort is required to prevent the above-mentioned drawbacks.

Fig. 1b, shows a TEM image of Cu-NPs-PEI(capping) corresponding to a micrograph section in Fig. 2c. The image clearly revealed the interplanar distance related to the planes (111) of $2.13 \pm 0.04 \text{ \AA}$, with cubic structure (ICDD reference code 00-001-1242). These results are relevant because the analysis indicates the electron transparency of the samples. HRTEM analyses do not reveal the structure of the core-shell or the CuO (coating) on the Cu-NPs surface. The size of the nanoparticles was approximately 5 nm, and nanoparticle sizes are larger than 8 nm were not found

in these analyses. Although the capping agent was not observed by the characterization techniques used, it is evident that the polymer in the solution avoids the aggregation process of the particles and plays an important role in the nucleation and growth process. As a result, Fig. 1c, which reveals small and homogeneous Cu-clusters with great dispersion, indicates that the blue-shift of the maximum absorption in the spectra of Fig. 1d is due to quantum size effects. It is also possible that Cu-NPs without PEI capping exhibit a red-shift because of the aggregation process.

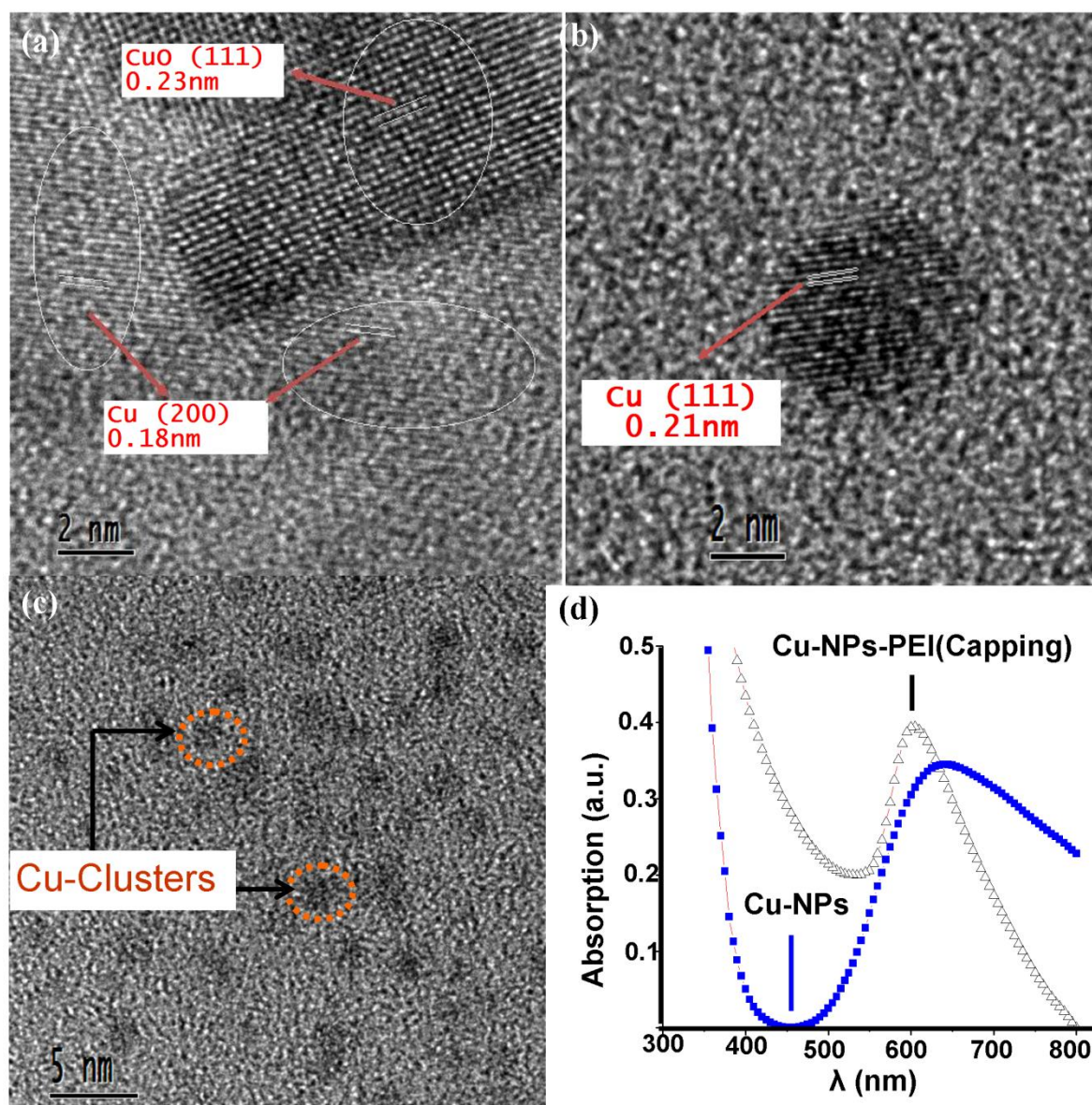


Fig. 1. HRTEM images a, b) an interface region of the Cu-NPs-PEI(capping) and without PEI, respectively. c) Cu-Clusters-PEI (capping) with narrow particle distribution. d) UV-Vis absorption spectra of Cu-NPs. The highest absorption corresponds to Cu-NPs (filled triangles) with capping and the other one corresponds to Cu-NPs-PEI(capping) (open triangles).

The Au-NPs without PEI are shown in Figs. 2a and 2b; in this case, larger aggregates of nanoparticles were found with different sizes and shapes, with the principal characteristic of these particles being its high crystallinity. The Au-NPs crystalline can be explained by the synthesis technique used: because of the high energy of the photons of the laser light illuminating the Au target and because it produces an excess energy in a very short time (5 ns); this excess energy is

adsorbed with high efficiency by the nanoparticles dispersed in the solution. The above process facilitates the atoms packing to form crystalline structures. Au-NPs-PEI(capping) clearly exhibited a preferential crystallographic orientation of five-fold symmetry that is characteristic of icosahedral, cuboctahedral and decahedral geometries [7]. In Fig. 2c, one can observe Au icosahedral nanoparticles with three-fold symmetry; the interplanar distances were resolved with good contrast, and their surface facets are identified. The interplanar distance found were 2.42 Å and 1.47 Å, which correspond to the (111) and (220) planes, respectively. These particles exhibited, as those of Cu, a small blue-shift in the UV-Vis spectrum, as shown in Fig. 2d. The difference between of the separation of absorption bands in the Au- and Cu-NPs-PEI(capping) spectra indicates that the size dispersion of Cu-NPs is higher than that of the Au-NPs.

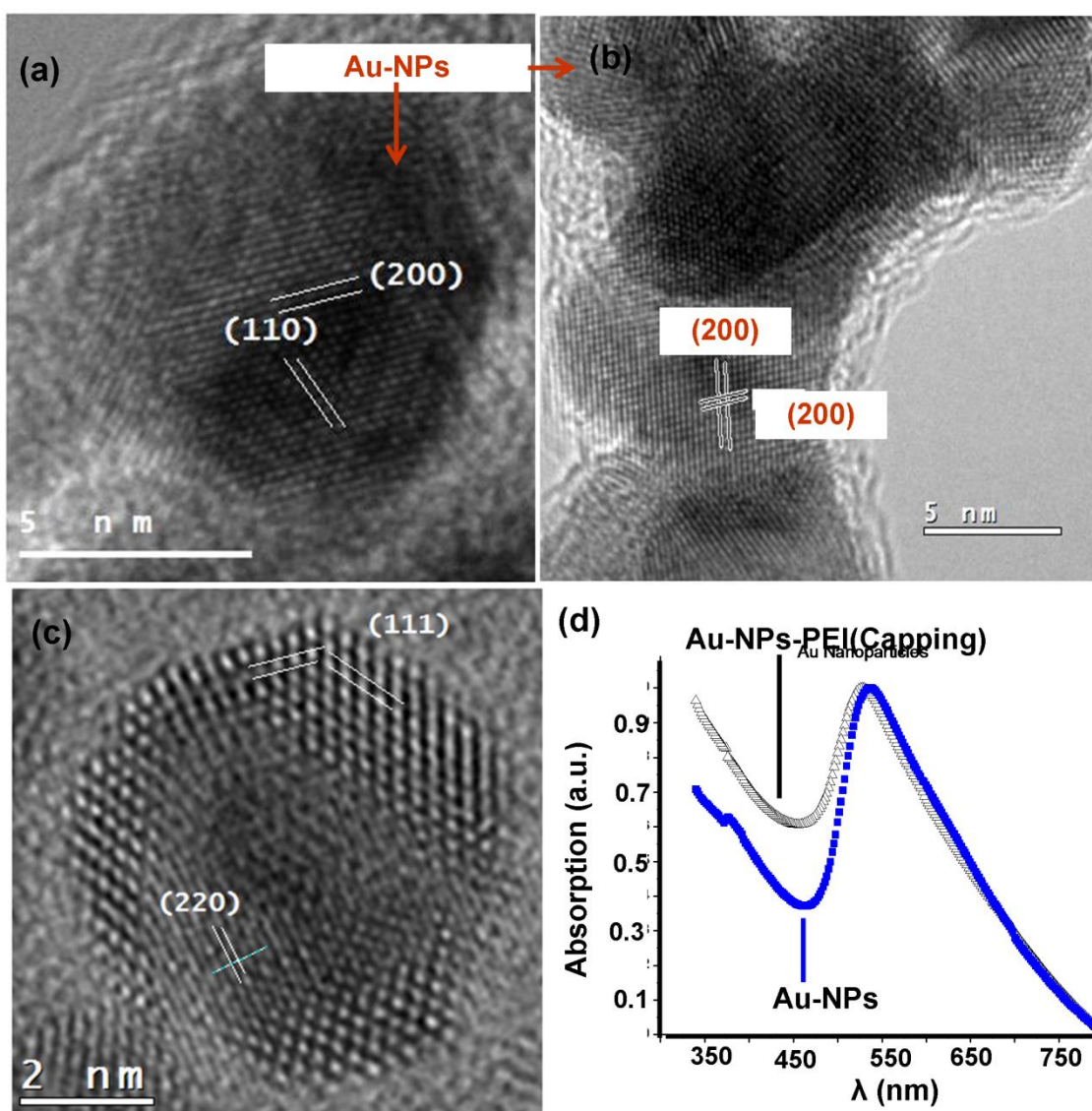


Fig. 2. HRTEM images a, b) Au-NPs without capping. c) Au-NPs-PEI(capping), with five fold orientations. d) UV-Vis absorption spectra of Au-NPs. The highest absorption corresponds to Au-NPs (filled triangles), the other one corresponds to Au-NPs-PEI(capping) (open triangles)..

Two micrographs of Au-NPs-PEI(capping) with five-fold symmetry are shown in Figs. 3a and 3b: the particles in these images have an optimal shape, size and geometry control. This optimal nanoscale control is very important because the control of the above-mentioned

parameters are fundamental to design devices, whose optical, electrical and other properties do not significantly change from device to device. Various authors, such as Barnard [38], suggest a new Au phase diagram in the nanometer scale that explains to some extent the high stability of the Au-NPs' icosahedral shape; based on this phase diagram, many authors have attempted to use these systems to control the nanoparticle growth to obtain a narrow particle distribution [39-41]. In addition, in this work, the formation of small nanoparticles of size of 2 nm, which are sometimes called clusters, was observed. The number of atoms on their surface considerably modifies the properties of clusters. Clusters also exhibit isomerism and high chemical reactivity due to the high relative percentage of atoms on the surface of greater than 50%. The clusters have low crystal stability, which explains the diversity of crystalline structures with the same number of atoms. Therefore, the energy difference between two structures with the same number of atoms is very small [42-46]. Fig. 3c shows two Au clusters at approximately 1.5 nm; it is therefore suggested that the synthesis by pulsed laser ablation promotes or encourages Au clusters of defined geometry and of high stability configurations[47-48].

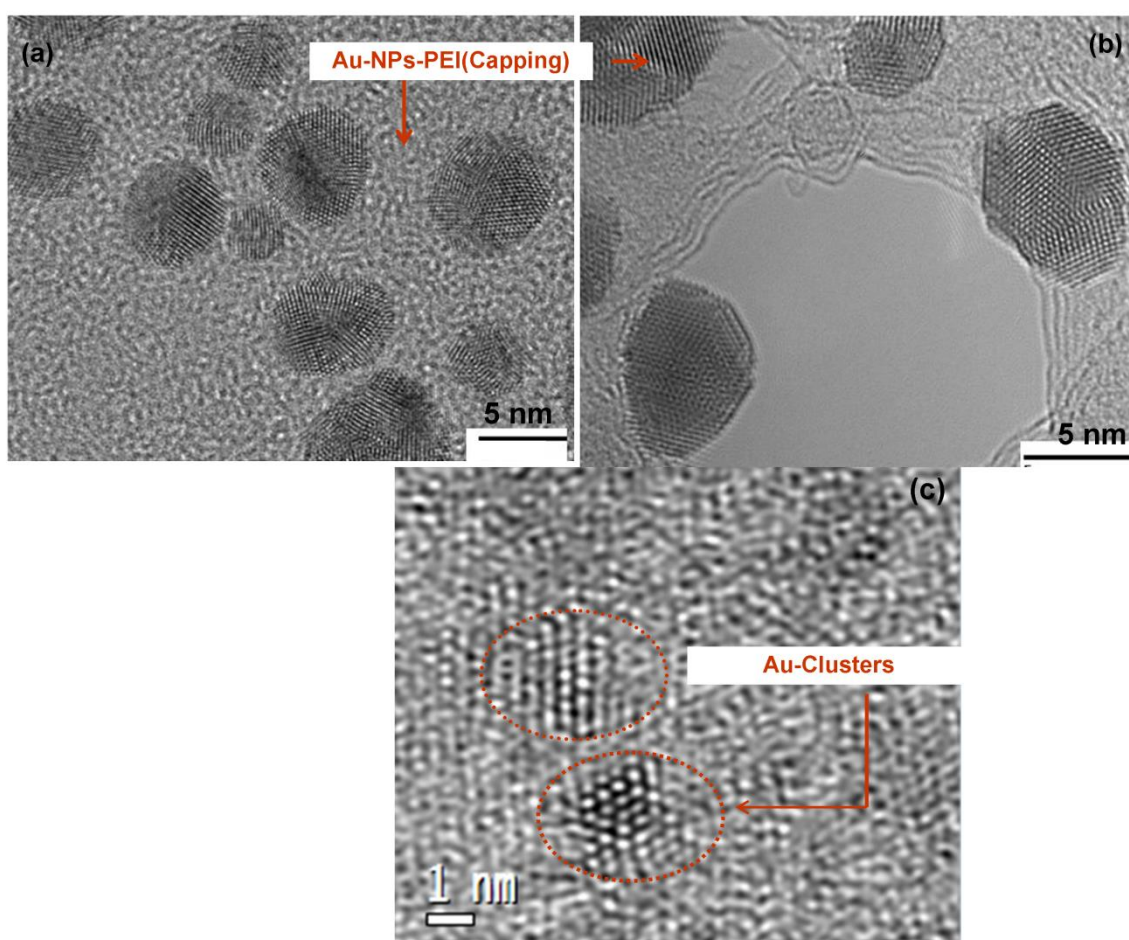


Fig. 3. HRTEM images a), b) of the Au-NPs-PEI(capping), with five fold orientations. b) Au-Clusters-PEI(capping).

2.2.2 Optical Study

The effect of PEI capping on the optical properties of Au-NPs was studied using UV-Vis spectroscopy (see Fig. 2d). The Au-NPs exhibited an absorption edge at ~ 536 nm, which is consistent with the previously reported spectra for these particles [49]. In contrast, Au-NPs-PEI(capping) exhibited a wide absorption symmetric peak at ~ 526 nm, as was commented in the previous sections; the Au surface protected with the capping agent avoids the aggregation process and the nucleation is also controlled, thereby leading to the lower particles sizes. The narrow

particles distribution and the small size of the Au-NPs-PEI(capping) produce a slight blue-shift because of quantum size effects. The same phenomenon occurs with Cu-NPs-PEI(capping) (Fig. 1d). The blue-shift is more pronounced in the Cu-NPs with capping than in the Au-NPs-PEI(capping), which could be due to the major size control via spherical stabilization. This control can be seen in fig. 1a, by comparing the Cu-NPs with capping agent with those of Au shown in Fig. 3a. Cu-NPs without PEI capping exhibit a strong absorption at 639 nm that is characteristic of the surface plasmon [49-50]; in the case of Cu-NPs-PEI(capping), an asymmetric band at 605 nm in the spectra was observed. This effect has been published before by many authors, who indicated that surface plasmon band due to collective excitations of the free electron [50-51]. is responsible for this band. Moreover, the Cu-NPs-PEI(capping) exhibited a broad absorption from 50 to 800 nm; this behavior can be explained by inter band transitions. In the same way, the broad absorption at approximately 800 nm is due to the d-d band transitions of ions Cu^{2+} ; perhaps these ions can be produced in the single surface layer by adsorption of the dissolved oxygen in the water media or by hydroxide ions adsorption derived from the aqueous media.

2.2.3 Zeta Potential (ZP)

The Zeta potential (ZP) results (see table 1) clearly revealed the PEI capping effect on the Cu- and Au-NPs. For Au-NPs without PEI capping, the ZP was -24.23 mV, similar to previous reports [47, 48, 52], suggesting that these nanoparticles dispersed in water generally exhibit negative ZP values due to hydroxide ions adsorption from the aqueous media. For Au-NPs-PEI(capping), the ZP value was 12.54 mV, similar to previous reports [48]. In the case of Cu-NPs without PEI capping, the ZP value was -97.59 mV; the high negative values can be explained by the high reactivity of the Cu-NPs, which in water media react to produce CuO (II). Similar oxidation occurs in the Ti-NPs, where high surface reactivity lead to a change of Ti to TiO_2 nanoparticles only in 30 min [37]. In the Cu-NPs surface, the oxidation starts, and this continues by oxygen diffusion in the particles, as seen in Fig. 1a, which shows the interface between Cu and CuO-NPs. The ionic bonding of CuO-NPs produce a surface with high potential that enables the absorption of hydroxide ions and water molecules, which can explain the high ZP values exhibited by these particles. Another possible explanation may be related with the high stability of the largest aggregates of Cu-NPs (see Fig. 1) because they can produce a Cu colloidal stable solution without PEI capping. Cu-NPs-PEI(capping) exhibited a ZP value of -0.64 mV; this negative value can indicate the incomplete capping of the Cu-NPs surface. These results are relevant because the HRTEM indicated the electron transparency of these samples, indicating that it is possible that not all surface is functionalized with PEI. Therefore, HRTEM analyses do not reveal the formation core-shell structure as Cu/CuO in the surface of Cu-NPs-PEI(capping) and do not reveal the PEI capping on the nanoparticle surface.

Table 1. Effect of the PEI capping on Cu-NPs and Au-NPs.

| NPs/Cluster | Zeta Potential (mv) | Size by TEM (nm) | Size by Zeta Potential (nm) | UV-Vis Absorbance (nm) |
|----------------------|---------------------|---------------------|--|------------------------|
| Au-NPs | -24.23 | $\geq 5\text{nm}$ | $\geq 5\text{nm}$ | 536 |
| Au-NPs-PEI(capping)* | 12.54 | $\leq 4.5\text{nm}$ | $\leq 4.0\text{nm}$ and large aggregates | 527 |
| Cu-NPs | -97.59 | $\geq 6\text{nm}$ | 1.5 | 639 |
| Cu-NPs-PEI(capping)* | -0.64 | $\leq 10\text{nm}$ | Large Aggregates | 605 |

*In both cases were found size cluster with size smaller than 2nm.

3. Conclusions

Cu- and Au-NPs with average sizes of approximately 5.0 nm, and Au- and Cu-NPs-PEI(capping) with sizes smaller to 2.0 nm were synthesized using pulsed laser ablation in water media. The narrow size distribution was determined by the techniques of HRTEM and DLS. The

addition of the polymer capping was demonstrated to prevent the aggregation or coalescence process of the nanoparticles. The Cu-NPs without PEI capping eases the CuO formation caused by the high reactivity of Cu-NPs due to its high surface energy and by the fast oxygen diffusion on the Cu-NPs surface. The Cu-NPs-PEI(capping) are spherically stabilized and were found to avoid aggregation and flocculation. Zeta Potential values different from zero indicated the incomplete PEI capping over the entire surface; nevertheless, the PEI capping is sufficient to prevent oxidation of Cu-NPs. Au-NP particles exhibited high crystallinity without PEI capping, but the formation of large aggregates with high crystallinity were observed. In contrast, Au-NPs-PEI(capping) exhibited the five-fold orientation preferential as icosahedral symmetry, cuboctahedral and decahedral geometry. This symmetry is very relevant because the optimal shape, size and geometry control of nanostructure is the most essential point in the design and fabrication of devices using nanoparticles. The functionalized surface with the capping agent in this synthesis helped to some extent to obtain dispersed nanoparticles. Au-PEI clusters of size of less than 1.5 nm with defined geometry and of high stability configuration were observed. The formation of such clusters is driven by the thermodynamic and chemical environment control (the addition of capping agents). Finally, a new route to produce Au-NPs, Cu-NPs and clusters functionalized with PEI was proposed.

Acknowledgements

The project described was supported by Award Number (168813 & 234104) from CONACYT, México. The content is solely the responsibility of the authors and does not necessarily represent the official views of the CONACYT. PROMEP program (grant number 103.5/10/6135 UANL-México) and also to PAICYT-UANL grant number (CE784-11). The authors thank to electronic microscopy laboratory of the International Center for Nanotechnology and Advanced Materials from University of Texas at San Antonio (UTSA) and we also thank to Department of Materials Engineering (DIMAT) of the University of Concepción, Chile.

References

- [1] V. F Puentes, K.M Krishnan, P Alivisatos *Science*. **291**, 2115 (2011)
- [2] G.A Somorjai, J.Y Park. *Top. Catal.* **49**, 126 (2008)
- [3] H Lara, L Ixtepan-Turrent, E Garza-Treviño, C Rodriguez-Padilla *J. Nanobiotechnology*. **8**,18. (2010)
- [4] G Rodriguez-Gattorno, D Diaz, L Rendon, G.O Hernandez-Segura, *J. Phys. Chem. B*. **106**, 2482 (2002)
- [5] C Urda, X.B Chen, R Narayanan, M.A El-Sayed, *Chem. Rev.* **105**, 1025 (2005)
- [6] N.A. Ramos-Delgado, L. Hinojosa-Reyes, J.L. Guzmán-Mar M.A. Gracia-Pinilla, A. Hernández-Ramírez, *Catalysis Today*. **209**, 35 (2013)
- [7] I. Medina-Ramírez, J. L. Liu, A., A. Hernández-Ramírez, C. Romo-Bernal, G. Pedroza-Herrera, J. Jáuregui-Rincon, M.A. Gracia-Pinilla, *J. Mater. Sci.***49**, 5309 (2014).
- [8] P Sathishkumar, R. V.Mangalaraja, O. Rosaz, H. D. Mansilla, M.A. Gracia-Pinilla, M. F. Meléndrez, S. Anandan, *Separation and Purification Technology*. **113**, 407 (2014)
- [9] J. H Kim, T. A Germer, G. W Mulholland, S. H Ehrman, *Adv. Mater.* **14**, 518 (2002).
- [10] I.M Goldby, B VonIssendorff , L Kuipers, R.E Palmer *Rev. Sci. Instrum.* **68**, 3327 (1997)
- [11] J. A de Toro, J.P Andrés, J.A González, J. M Riveiro, M Estrader, A López-Ortega, I Tsiaoussis, N Frangis, J Nogués. *J. Nanopart. Research*. **13**, 4583 (2012).
- [12] K. A Homan, M Souza, R Truby, G. P Luke, C Green, E Vreeland, S Emelianov *ACS Nano*. **6**, 641 (2012)
- [13] T Ling, L Xie, J Zhu, H Yu, H Ye, R Yu, Z Cheng, L Liu, G Yang, Z Cheng, Y Wang, X Ma *NanoLett.* **9**, 1572 (2009)
- [14] R.W.J Scott, O.M Wilson, R.M Crooks *J. Phys. Chem. B*. **109**, 692 (2005)
- [15] T. C Wang, M. F Rubner, R. E Cohen, *Langmuir*.**18**, 3370 (2002).

- [16] F Mafuné, J Kohno, Y Takeda, T Kondow, H Sawabe *J. Phys. Chem. B.* **104**, 9111. (2000)
- [17] E Haro-Poniatowski, M Jouanne, J.F Morhange, M Kanehisa, R Serna, C.N Afonso *Phys. Rev. B.* **60**, 10080 (1999).
- [18] V.M Serdio, M.A Gracia-Pinilla, S Velumani, E Perez, W.V.D Wiel, *J. Nanoresearch.* **9**, 101 (2010).
- [19] N.A. Ramos-Delgado, M.A. Gracia-Pinilla, L. Maya-Treviño, L. Hinojosa-Reyes, J.L. Guzmán-Mar, A. Hernández-Ramírez, *J. Hazardous. Materials.* **263**, 36 (2013)
- [20] A Tlahuice, I.L Garzón, *Phys. Chem. Chem. Phys.* **14**, 7321 (2012)
- [21] K Michaelian, N Rendón, I.L Garzón, *Phys. Rev. B.* **60**, 2000 (1999)
- [22] I.L Garzón, K Michaelian, M.R Beltrán, A Posadas-Amarilas, P Ordejon, E Artacho, D Sanchez-Portal, J.M Soler, *Phys. Review. Lett.* **81**, 1600. (1999)
- [23] F Baletto, R Ferrando, A Fortunelli, F Montalenti, C Mottet, *J. Chem. Phys.* **116**, 3856 (2002)
- [24] V Švrček, D Mariotti, K Kalia, C Dickinson, M Kondo, *J. Phys. Chem. C.* **115**, 6235 (2011)
- [25] M José-Yacamán, C Gutierrez-Wing, M Miki, D.Q Yang, K. N Piyakis, E Sacher, *J. Phys. Chem. B.* **109**, 9703 (2005).
- [26] T. H. Lim, D. McCarthy, S. C. Hendy, K. J. Stevens, S. A. Brown and R. D. Tilley. *ACS Nano.* **3**(11), 3809 (2009).
- [27] W. J. Song, J. Z. Du, T. M. Sun, P. Z. Zhang, P. Zhuo, W. Jun. *Small.* **6**, 239 (2010).
- [28] D.A. Elbakry, A. Zaky, R. Liebl, R. Rachel, A. Goepferich, M. Breunig. *Nano. Lett.* **9**(5), 2059 (2009).
- [29] G. Han, P. Ghosh, V. M. Rotello. *Nanomedicine-UK.* **2**(1), 113 (2007).
- [30] H. Parab, C. Jung, M. A. Woo, H. G. Park. *J. Nanopart. Res.* **13**(5), 2173 (2011).
- [31] C. Hu, Q. Peng, F. Chen, Z. Zhong, R. Zhuo. *Bioconjugate Chem.* **21**(5), 836 (2010).
- [32] M. Kawasaki. *J. Phys. Chem. C.* **115**(12), 5165 (2011).
- [33] D. Amans, C. Malaterre, M. Diouf, C. Mancini, F. Chaput, G. Ledoux, G. Breton, Y. Guillin, C. Dujardin, K. Masenelli-Varlot, P. Perriat. *J. Phys. Chem. C.* **115**(12), 5131 (2011).
- [34] T. E. Itina. *J. Phys. Chem. C.* **115**(12), 5044 (2011).
- [35] M. Muniz-Miranda, C. Gellini, E. Giorgetti. *J. Phys. Chem. C.* **115**(12), 5021 (2011).
- [36] H. Muto, K. Yamada, K. Miyajima, F. Mafuné. *J. Phys. Chem. C.* **111**(46), 17221 (2007).
- [37] S. Ibrahimkuty. M. Gopinadhan, C. A. Helm, B. M. Smirnov, R. Hippler. *Thin Solid Films.* **500**(1-2), 41 (2006).
- [38] A. S. Barnard, N. P. Young, A. I. Kirkland, M. A. van Huis, H. Xu. *ACS Nano.* **3**(6), 1431 (2009).
- [39] J.P.K. Doye, F. Calvo. *Phys. Rev. Lett.* **86**(16), 3570 (2001).
- [40] F. Baletto, C. Mottet, R. Ferrando. *Phys. Rev. Lett.* **84**(24) 5544 (2000).
- [41] S. Iijima, T. Ichihashi. *Phys. Rev. Lett.* **56**, 616 (1986).
- [42] P. M. Ajayan, L.D. Marks. *Phys. Rev. Lett.* **60**, 585 (1988).
- [43] L.D. Marks. *Rep. Prog. Phys.* **57**, 603 (1994).
- [44] P. Buffat, M. Flüeli, R. Spycher, P. Stadelmann, P. Borel. *Faraday Discuss.* **92**, 173 (1991).
- [45] X. Xing, R.M. Danell, I.L. Garzón, K. Michaelian, M.N. Blom, M. M. Burns, J.H. Parks. *Phys. Rev. B.* **72**, 081405 (2005).
- [46] D. Reinhard, B.D. Hall, D. Ugarte, R. Monot. *Phys. Rev. B.* **57**, 7868 (1997).
- [47] T. Kim, K. Lee, M-S. Gong, S-W. Joo. *Langmuir.* **21**, 9524 (2005)..
- [48] C. Hu, Q. Peng, F. Chen, Z. Zhong, R. Zhuo. *Bioconjugate Chemistry* **21**(5) 836 (2010).
- [49] M Kawasaki *J. Phys. Chem. C.* **115**, 5165 (2011).
- [50] P. Sathishkumar, R.V. Mangalajara, H.D. Mansilla, M.A. Gracia-Pinilla, S. Anandan. *Applied. Catalysis. B.* **160-161**, 692 (2014).
- [51] C. Salzemann, I. Lisiecki, A. Brioude, J. Urban, M.P. Pileni. *J. Phys. Chem. B* **108** (35), 13242 (2004).
- [52] T.L. Doane, C-H. Chuang, R.J. Hill, C. Burda. *Accounts Chem. Res.* **45**(3) 317 (2012).